IAI Journals.ASM.org

Beyond the Crystal Structure: Insight into the Function and Vaccine Potential of TbpA Expressed by *Neisseria gonorrhoeae*

Devin R. Cash,[a] Nicholas Noinaj,[b]* Susan K. Buchanan,[b] Cynthia Nau Cornelissen[a]

Department of Microbiology and Immunology, Virginia Commonwealth University, Richmond, Virginia, USA[a]; Laboratory of Molecular Biology, NIDDK, National Institutes of Health, Bethesda, Maryland, USA[b]

***Neisseria gonorrhoeae*, the causative agent of the sexually transmitted infection gonorrhea, is not preventable by vaccination and is rapidly developing resistance to antibiotics. However, the transferrin (Tf) receptor system, composed of TbpA and TbpB, is an ideal target for novel therapeutics and vaccine development. Using a three-dimensional structure of gonococcal TbpA, we investigated two hypotheses, i.e., that loop-derived antibodies can interrupt ligand-receptor interactions in the native bacterium and that the loop 3 helix is a critical functional domain. Preliminary loop-derived antibodies, as well as optimized second-generation antibodies, demonstrated similar modest ligand-blocking effects on the gonococcal surface but different effects in *Escherichia coli*. Mutagenesis of loop 3 helix residues was employed, generating 11 mutants. We separately analyzed the mutants' abilities to (i) bind Tf and (ii) internalize Tf-bound iron in the absence of the coreceptor TbpB. Single residue mutations resulted in up to 60% reductions in ligand binding and up to 85% reductions in iron utilization. All strains were capable of growing on Tf as the sole iron source. Interestingly, in the presence of TbpB, only a 30% reduction in Tf-iron utilization was observed, indicating that the coreceptor can compensate for TbpA impairment. Complete deletion of the loop 3 helix of TbpA eliminated the abilities to bind Tf, internalize iron, and grow with Tf as the sole iron source. Our studies demonstrate that while the loop 3 helix is a key functional domain, its function does not exclusively rely on any single residue.**

Neisseria gonorrhoeae, the causative agent of the sexually transmitted infection gonorrhea (1), affects approximately 106 million people worldwide according to WHO estimates (2), with >300,000 cases of gonorrhea reported each year in the United States alone (3). A troubling contributor to these statistics is that infection with this bacterium does not result in any protective immunity (4). Additionally, approximately 50% of the women infected with the gonococcus are asymptomatic, resulting in increased spread and more severe clinical outcomes following infection (5). Most concerning of all is that the gonococcus has become increasingly drug resistant, with mounting evidence to suggest that current pharmacotherapies may soon be rendered obsolete (6, 7). To date, the characteristics of at least three multidrug-resistant isolates have been published, all of which are fully resistant to ceftriaxone, the core component of the currently recommended combination therapy for the treatment of gonorrhea (7–11). With dwindling treatment options and no vaccine, gonorrhea is a serious public health concern that warrants further research.

One approach to the development of therapeutics has been to study how the gonococcus acquires iron, an essential nutrient for nearly all microorganisms (12). During human infection, microorganisms are confronted with the challenge of obtaining iron in an environment that has evolved to specifically restrict its availability. In humans, iron is circulated throughout the body bound to several transport proteins, including lactoferrin and transferrin (Tf). These iron binding proteins minimize free iron concentrations, which helps to reduce free radical generation, as well as starve any invading microbes. In response to this iron limitation, many bacteria produce siderophores to compete with these human proteins for iron (13). However, *N. gonorrhoeae* has evolved the ability to acquire iron directly from these human proteins.

The gonococcus expresses receptors that can extract iron or heme from Tf, lactoferrin, and hemoglobin, but the receptors are not universally expressed (14, 15). The lactoferrin receptor proteins, LbpA and LbpB, are expressed in only approximately 50% of strains (16, 17). The hemoglobin receptor proteins, HpuA and HpuB, are expressed only in isolates from women in the first half of the menstrual cycle because of phase variation (18). In contrast, the Tf receptor system composed of an integral, outer membrane, TonB-dependent transporter, TbpA, and a surface-exposed lipoprotein, TbpB, is expressed in 100% of clinical isolates (19). This set of human-adapted receptors has made the gonococcus well suited to survive in the iron-limited environment of the human host.

Iron acquisition systems are potential targets for novel drug therapies, as well as for vaccine development. Because the gonococcal Tf receptors are not subject to phase or antigenic variation, are present in all clinical isolates, and are necessary for initiation of infection in humans (20), they stand out as ideal candidates for further investigation. Much work has already been done to probe this receptor complex for structure-function relationships and vaccine potential (14, 15, 19). Recently, the Tf receptors, TbpA

Received 9 June 2015 **Returned for modification** 29 June 2015
Accepted 31 August 2015

Accepted manuscript posted online 8 September 2015

Citation Cash DR, Noinaj N, Buchanan SK, Cornelissen CN. 2015. Beyond the crystal structure: insight into the function and vaccine potential of TbpA expressed by *Neisseria gonorrhoeae*. Infect Immun 83:4438–4449. doi:10.1128/IAI.00762-15.

Editor: C. R. Roy

Address correspondence to Cynthia Nau Cornelissen, cncornel@vcu.edu.

* Present address: Nicholas Noinaj, Purdue University, West Lafayette, Indiana, USA.

Supplemental material for this article may be found at http://dx.doi.org/10.1128/IAI.00762-15.

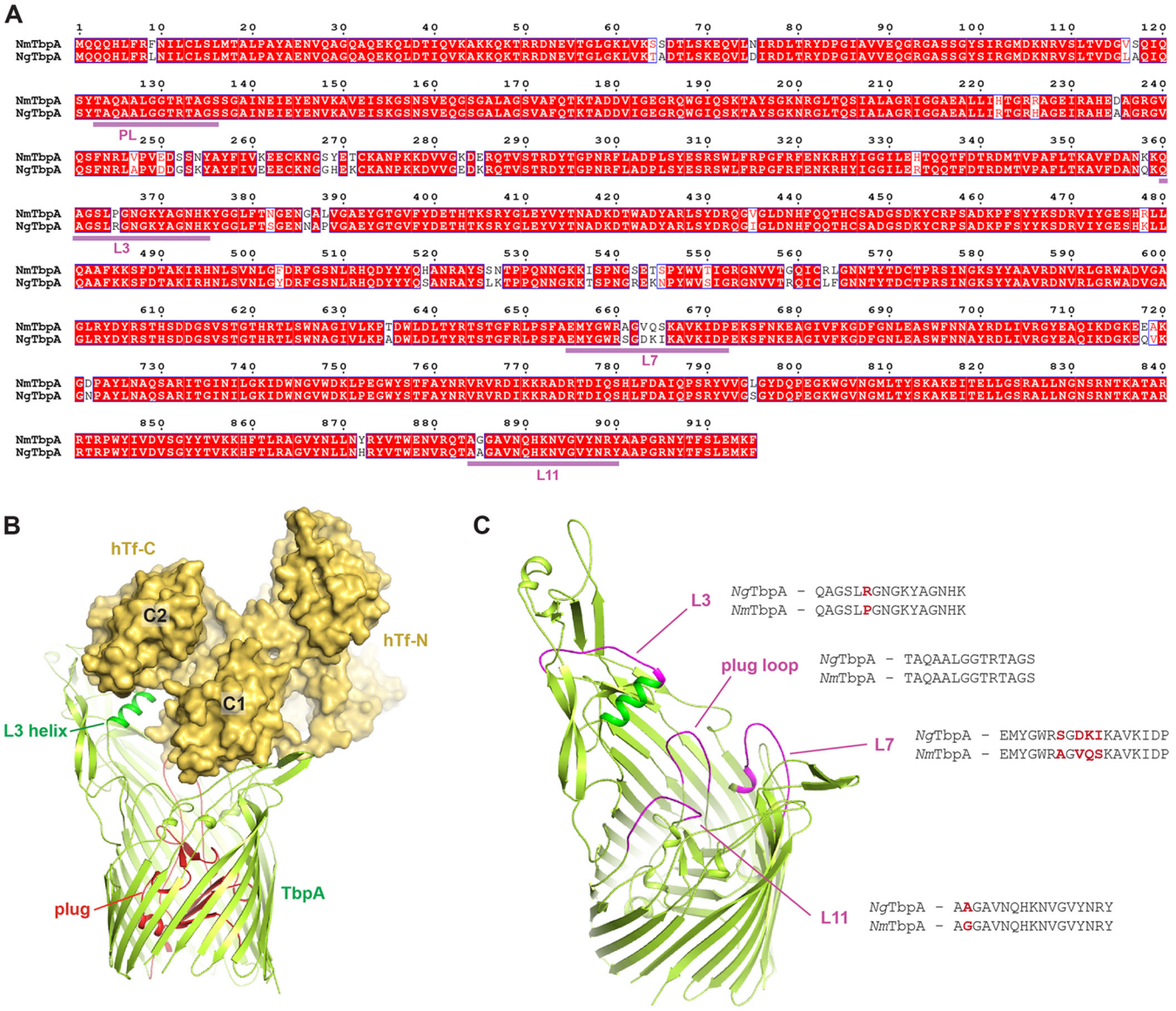

FIG 1 Homology model for TbpA from gonococcal strain FA19. (A) Alignment of the sequences of the TbpA proteins of *N. meningitidis* strain K454 (NmTbpA) and *N. gonorrhoeae* strain FA19 (NgTbpA), which are 94% identical, with loop 3 (L3), L7, and L11 and the plug (PL) underlined. This alignment served as the basis for homology modeling of TbpA from strain FA19. (B) On the basis of the complex crystal structure with NmTbpA, hTf (hTf-C/hTf-N) (shown in gold) was modeled interacting with NgTbpA (shown in light green), with the plug domain shown in red and the L3 helix shown in dark green. The C1 and C2 domains of the C lobe of hTf, which directly interact with TbpA, are also indicated. (C) L3, L7, L11, and part of the plug domain were selected for initial blocking studies with antibodies against TbpA from strain K454. Highlighted in magenta are the conserved regions of the NgTbpA model to which those antibodies were developed. Pairwise comparisons of the peptide sequences are also shown.

and TbpB, were crystallized from the closely related pathogen *Neisseria meningitidis*; they show 94 and 69% identity with the respective proteins in *N. gonorrhoeae* strain FA19 (21, 22). The structural studies provided the molecular details of how these receptors interact with Tf and will significantly contribute to the study of these proteins for therapeutic development. On the basis of the structure of TbpA, experiments were performed to test various surface-exposed epitopes as immunogens and to determine if antibodies raised against these regions could interrupt protein function (21). The results of these studies were promising; however, they were performed with recombinant *N. meningitidis* TbpA in an *in vitro* assay. Here, we follow up these studies to test the degree to which these antibodies inhibit ligand binding to TbpA in the native bacterium *N. gonorrhoeae*. Further, we developed our own loop-specific antibodies in an attempt to improve their inhibitory efficiency. To probe the structure-function relationships of this receptor, we built on previous work to target the TbpA loop 3 helix, a motif located in close proximity to the iron chelation center within the C-lobe cleft of Tf (Fig. 1). On the basis of the TbpA crystal structure and previous evidence that interruption of loop 3 led to a loss of protein function (23), this motif is predicted to be a key to protein function. To assess the contribution of the loop 3 helix to protein function, site-specific mutagenesis of polar residues, fol-

TABLE 1 Bacterial strains used in this study

Strain	Description	Source
E. coli		
BL21(DE3)	*fhuA2* [*lon*] *ompT gal* (λ DE3) [*dcm*] Δ*hsdS* λ DE3 = λ sBamHIo ΔEcoRI-B *int*::(*lacI*::P_{lacUV5}::T7 gene1) *i21* Δ*nin5*	New England Biolabs
C41(DE3)	F^- *ompT* $hsdS_B$(r_B^- m_B^-) (r_B^- m_B^-) *gal dcm* (DE3) uncharacterized derivative of BL21(DE3)	Lucigen
Top10	F^- *mcrA* Δ(*mrr-hsdRMS-mcrBC*) ϕ80*lacZ*ΔM15 Δ*lacX74 recA1 deoR araD139* Δ(*ara-leu*)*7697 galU galK rpsL*(Str^r) *endA1 nupG*	Invitrogen
XL-10 Gold	*endA1 glnV44 recA1 thi-1 gyrA96 relA1 lac* Hte Δ(*mcrA*)*183* Δ(*mcrCB-hsdSMR-mrr*)*173* Tet^r F′ [*proAB* $lacI^qZ$ΔM15 Tn*10*(Tet^r Amy^r Cm^r)]	Agilent Technologies
N. gonorrhoeae		
FA19	Wild type	49
FA6747	$TbpA^-$ (*tbpA*::mTn*3cat*)	29
FA6905	$TbpB^-$ (Δ*tbpB*)	36
FA6815	$TbpAB^-$ (*tbpB*::Ω)	32
MCV511	$L3HA_{(343)}$ TbpA Lbp^- (*tbpA*∇HA *lbpB*::Ω)	23
MCV512	$L3HA_{(343)}$ TbpA $TbpB^-$ Lbp^- (*tbpA*∇HA *lbpB*::Ω Δ*tbpB*)	23
MCV161	TbpA K351A point mutation $TbpB^-$ (Δ*tbpB*)	This study
MCV162	TbpA D355A point mutation $TbpB^-$ (Δ*tbpB*)	This study
MCV163	TbpA D355K point mutation $TbpB^-$ (Δ*tbpB*)	This study
MCV164	TbpA N357A point mutation $TbpB^-$ (Δ*tbpB*)	This study
MCV165	TbpA Q358A point mutation $TbpB^-$ (Δ*tbpB*)	This study
MCV166	TbpA K359A point mutation $TbpB^-$ (Δ*tbpB*)	This study
MCV167	TbpA K359E point mutation $TbpB^-$ (Δ*tbpB*)	This study
MCV168	TbpA K359R point mutation $TbpB^-$ (Δ*tbpB*)	This study
MCV169	TbpA Q360A point mutation $TbpB^-$ (Δ*tbpB*)	This study
MCV170	TbpA Q360E point mutation $TbpB^-$ (Δ*tbpB*)	This study
MCV171	TbpA Q360K point mutation $TbpB^-$ (Δ*tbpB*)	This study
MCV172	TbpA loop 3 helix deletion (T350-A361) $TbpB^-$ (Δ*tbpB*)	This study
MCV181	TbpA K351A point mutation	This study
MCV182	TbpA D355A point mutation	This study
MCV183	TbpA D355K point mutation	This study
MCV184	TbpA N357A point mutation	This study
MCV185	TbpA Q358A point mutation	This study
MCV186	TbpA K359A point mutation	This study
MCV187	TbpA K359E point mutation	This study
MCV188	TbpA K359R point mutation	This study
MCV189	TbpA Q360A point mutation	This study
MCV190	TbpA Q360E point mutation	This study
MCV191	TbpA Q360K point mutation	This study
MCV192	TbpA loop 3 helix deletion (T350-A361)	This study

lowed by ligand binding and radiolabeled iron uptake assays, was employed. The mutants created were also tested for the ability to grow on Tf as the sole iron source.

The studies described here demonstrate that the original loop antibodies had only modest abilities to block ligand binding to TbpA. Similarly, newly generated loop-specific antibodies led to modest inhibition of ligand binding to TbpA. However, unlike the original antibodies, the newer antibodies had a greater effect on the gonococcus than in recombinant *Escherichia coli*. With regard to the loop 3 helix, reduction of TbpA function could be achieved with single amino acid mutations; however, the coreceptor, TbpB, could largely compensate for these defects in TbpA function. All singly mutated strains were capable of growth on poorly saturated Tf; however, a total helix deletion strain could not grow under these conditions. This work provides new insights into improved antibody development against TbpA loop peptides, which will enhance vaccine efforts going forward. This study also demonstrates that the entire loop 3 helix significantly contributes to TbpA function but that there is no single amino acid that is crucial. This information contributes to our expanding understanding of key ligand-interacting domains, which will likely be needed in order to optimize immunogen interaction with the host immune system during vaccination (24).

MATERIALS AND METHODS

Strains, plasmids, and media. All of the strains used in this study are described in Table 1; for all of the plasmids used, see Table S1 in the supplemental material. Plasmids were propagated in *E. coli* Top10 (Invitrogen) or XL-10 Gold (Agilent Technologies) cells. The strains used for pUNCH412 and pVCU757 expression were BL21(DE3) (New England BioLabs) and C41(DE3) (Lucigen), respectively. *E. coli* was cultured in Luria-Bertani broth in the presence of chloramphenicol (34 μg/ml) or ampicillin (200 μg/ml). Gonococcal cells were propagated on GC medium base (Difco) with Kellogg's supplement 1 (25) and 12 μM $Fe(NO_3)_3$ at 37°C with 5% atmospheric CO_2. When necessary, chloramphenicol was added to GC medium agar plates at a concentration of 1 μg/ml for selection of the resistance phenotype. For growth under iron-stressed conditions, gonococci were either grown on GC medium agar plates with the addition of 5 μM Desferal or cultured from GC medium agar plates into

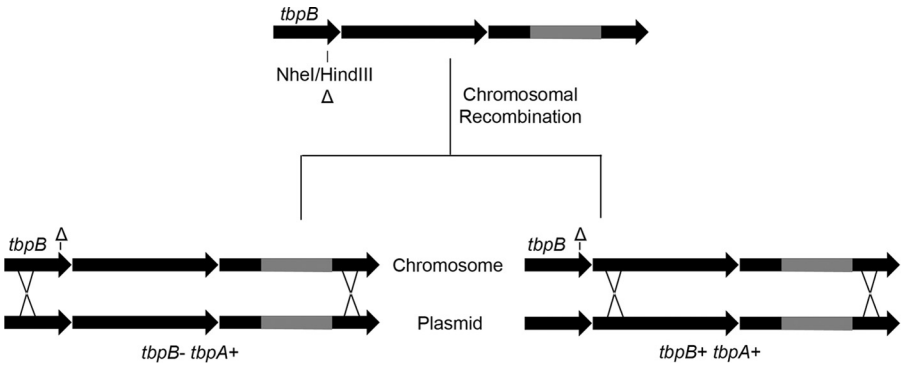

FIG 2 Gonococcal transformation with pUNCH755-derived plasmids pVCU161 to pVCU172. The image shown demonstrates how transformation with a single plasmid construct can result in two distinct genotypes following allelic exchange. The downstream crossover location is constrained by selection with chloramphenicol, whereas the upstream crossover can occur anywhere in *tbpA* or the truncated *tbpB* gene. If the crossover occurs upstream of the *tbpB* deletion, as shown on the left, the result is a $TbpB^-$ phenotype. Conversely, if the crossover occurs downstream of the deletion location, as shown on the right, the result is a $TbpB^+$ phenotype.

liquid chemically defined medium (CDM) (26) pretreated with Chelex 100 (Bio-Rad). CDM agar plates were supplemented with 2.5 μM 10% iron-saturated human Tf (Sigma) in order to assess each mutant's ability to utilize Tf-bound iron.

Modeling of TbpA from strain FA19. In order to model the structure of TbpA from gonococcal strain FA19, we performed homology modeling based on the structure of TbpA from *N. meningitidis* strain K454. Given that the two sequences were 94% identical with no gaps or insertions, a homology model was created with the SWISS-MODEL server (27) to thread the sequence of TbpA from FA19 onto the structure of TbpA from K454.

Solid-phase ligand-blocking assays. Solid-phase ligand-blocking assays were performed as previously described (28–30). Briefly, gonococcal strains were iron stressed in liquid CDM for 4 h and *E. coli* strains were grown in LB broth with 1 mM isopropyl-β-D-thiogalactopyranoside to induce TbpA expression. Bacteria were standardized to culture density and applied to a nitrocellulose membrane. Blots were blocked with 5% skim milk in low-salt Tris-buffered saline (LS-TBS; 50 mM Tris, 150 mM NaCl [pH 7.5]) for 1 h, washed five times with LS-TBS, and subsequently incubated with horseradish peroxidase (HRP)-tagged Tf (Jackson ImmunoResearch) at 200 ng/ml plus TbpA loop-specific mouse antiserum (21), polyclonal TbpA rabbit antiserum (unpublished), unlabeled human Tf (hTf; Sigma), or unlabeled bovine Tf (bTf; Sigma) for 1 h. Blots were washed five more times with LS-TBS and then developed with the Opti-4CN (Bio-Rad) development system.

Whole-cell ligand-blocking enzyme-linked immunosorbent assay (ELISA). MaxiSorp microtiter dishes (Nunc) were coated with 0.01% poly-L-lysine (Sigma) in phosphate-buffered saline (PBS) overnight at 4°C. Gonococci were iron stressed by overnight growth on GC medium agar plates containing 5 μM Desferal. Gonococcal cells were harvested from the agar plates and standardized to an optical density at 600 nm (OD_{600}) of 1.0 in PBS. One hundred microliters of the cell suspension was applied in triplicate for each strain and allowed to incubate on the plate for 1 h. The microtiter plate was washed five times with PBS, and then 200 μl of 3% bovine serum albumin (BSA) in PBS was added for 1 h of incubation. After the blocker was removed, antipeptide or anti-holo-TbpA serum was diluted 1:50 in 3% BSA and applied to the cells for 1 h of incubation, after which the cells were then washed five times with PBS. Then, 1 μg/ml HRP-Tf in 3% BSA was applied for 1 h incubation, which was followed by five washes with PBS. Subsequently, 100 μl of 1-Step Slow-TMB (Thermo) was added to colorimetrically detect the amount of HRP-Tf bound to the cells in each well. After 10 min, 100 μl of 2 M sulfuric acid was added to each well to stop the reaction. The OD_{420} of the microtiter plate was then read. Antibody blocking specificity was determined by performing these assays with bacterial strains without Tf receptor proteins (gonococcal strain FA6815 and *E. coli* expressing the empty vector) and subtracting these values from those of the experimental strains prior to normalization to the positive control.

Site-directed mutagenesis and cloning. Site-directed point mutations and deletions were constructed with the QuikChange system (Agilent). Briefly, the *tbpA* gene from strain FA19 was amplified and inserted into pHSS6-GCU (31) at the EcoRI restriction site. Subsequently, a silent BamHI restriction site was added adjacent to the DNA encoding the loop 3 helix. Mutagenic primers (sequences are available on request) were used to create point mutations, resulting in new plasmids with point mutations in *tbpA*. The resulting plasmids (pVCU150 to pVCU160) were then digested with ApaI and RsrII to obtain an approximately 870-bp region of *tbpA* containing the mutations. The pUNCH755 plasmid (Fig. 2), which contains a truncated *tbpB* gene, the full *tbpA* gene, and the *tbpA* downstream region containing a chloramphenicol resistance gene, was equivalently digested. The wild-type (WT) ApaI-RsrII *tbpA* region of pUNCH755 was replaced with the mutated ApaI-RsrII regions from plasmids pVCU150 to pVCU160, resulting in plasmids pVCU161 to pVCU171. *E. coli* Top10 cells were then transformed with the newly constructed plasmids, with selection for chloramphenicol resistance as already described.

Gonococcal transformation. Piliated gonococci were grown on GC medium agar plates. Cells were then transferred to GC medium plus Kellogg's supplement 1 and 10 mM $MgCl_2$. Bacteria were incubated with linearized plasmid DNA in liquid suspension and then plated on GC medium agar plates containing 1 μg/ml chloramphenicol. Since the new plasmids with mutated *tbpA* also contained a truncated *tbpB* gene, a single gonococcal transformation yielded colonies that had mutated TbpA with or without functional TbpB, depending on the distance between crossovers (see Fig. 2). Transformants were analyzed for the presence or absence of the complete *tbpB* gene by PCR. PCR amplification of *tbpA* was followed by restriction with BamHI to confirm that the mutagenized region was incorporated into the chromosome. The *tbpA* PCR products were also sequenced to confirm that the desired mutations were successfully incorporated into the gonococcal chromosome.

Tf binding ELISAs. Assays were performed in a manner similar to that described above for the whole-cell ELISA, except that the step in which antipeptide and anti-holo-TbpA antisera were added was omitted. HRP-Tf was used at concentrations ranging from 2 to 50 nM. A standard curve of HRP-Tf diluted in PBS was prepared by using concentrations ranging from 10 ng/ml to 1 μg/ml. Cell-containing wells were compared to the standard curve to determine the amount of Tf bound. Data were then normalized to the positive control. Graphs represent the data generated from at least three independent experiments done in triplicate.

Radiolabeled iron uptake assay. Tf-iron uptake assays were performed as described previously (32–35). Briefly, apo-human Tf (Sigma) was saturated to 20% with ^{55}Fe (Perkin-Elmer). Gonococci were iron stressed in liquid CDM for 3 h, and then 100 μl of the culture was applied in triplicate to two Millipore multiscreen microtiter dishes. Each microtiter well contained 1.5% BSA as a nonspecific protein blocker. One dish received 215 μM KCN to determine the counts bound but not internalized. Both plates were incubated for 10 min at 37°C and 5% CO_2. Subsequently, 3 μM 20% ^{55}Fe-saturated human Tf was added to each well and plates were again incubated for 30 min to allow iron internalization. Following incubation, each plate was filtered, washed, and dried and individual filters from each well were removed. Radioactive iron was detected with a Beckman LS6500 beta counter. All counts were averaged, and the surface-associated counts (KCN condition) were subtracted from the total counts to determine the amount of iron internalized in 30 min. Internalized iron was standardized to the number of micrograms of total cellular protein in 100 μl of culture, as determined by the BCA assay (Pierce). Final data are presented as values normalized to the positive control. Each graph represents the data generated from at least three independent experiments performed in triplicate.

Protease accessibility assay. Protease accessibility experiments were performed as described previously (36). Briefly, whole iron-stressed gonococci were exposed to trypsin for 0, 10, 20, or 30 min; pelleted; lysed; and subjected to Western blotting. Whole-cell pellets were resuspended in Laemmli solubilizing buffer and then supplemented with 5% β-mercaptoethanol. Samples were boiled for 3 min and then subjected to sodium dodecyl sulfate-polyacrylamide gel electrophoresis (SDS-PAGE). Following separation, proteins were transferred to nitrocellulose. For detection of TbpA, proteins were blocked with 5% BSA in high-salt TBS (20 mM Tris, 500 mM NaCl [pH 7.5], 0.02% NaN_3, 0.05% Tween 20). Blocked membranes were probed with polyclonal rabbit serum against full-length TbpA (29). Goat anti-rabbit IgG conjugated to alkaline phosphatase (AP) (Bio-Rad) was used as the secondary antibody. AP conjugates were detected with the nitroblue tetrazolium and 5-bromo-4-chloro-3-indolylphosphate development system (Sigma).

TbpA Western blotting. Whole iron-stressed gonococci were standardized to culture density, pelleted, and lysed. Cell lysates were resuspended in Laemmli solubilizing buffer, boiled for 3 min, subjected to a bicinchoninic acid protein assay (Thermo), supplemented with 5% β-mercaptoethanol, and then loaded equivalently by protein concentration onto a Criterion TGX polyacrylamide gel (Bio-Rad). Following separation by SDS-PAGE, proteins were transferred to nitrocellulose. Even protein loading was confirmed with staining with Ponceau S (Fisher). Immunodetection of TbpA was carried out as described above.

Statistics. Comparison of the results obtained with the positive control and mutant strains was performed after analysis of variance with the Student *t* test. Pairwise comparisons with a *P* value of <0.05 were considered statistically significant. The ELISA and radiolabeled iron uptake assay results shown are the means of multiple individual concentration points from studies performed at least in triplicate (± the standard error of the mean).

RESULTS

Antibodies raised against linear TbpA loop peptides minimally inhibit ligand binding to gonococcal whole-cell surface. A recent study (21) reported the crystal structure of TbpA from *N. meningitidis* and identified surface-exposed loops that facilitated substantial interaction with human Tf (Fig. 1). Linear peptide domains from several interactive loops were used as antigens in mice, and the subsequently produced sera were applied to *E. coli* strains expressing recombinant meningococcal TbpA. In recombinant *E. coli*, these antibodies were individually capable of blocking human Tf binding by approximately 50%; however, the previous study did not address whether the antibodies were capable of direct interaction with TbpA in whole *Neisseria* cells (21). To investigate this in *N. gonorrhoeae*, we first used the structure of TbpA from *N. meningitidis* strain K454 to create a homology model of TbpA (Fig. 1). Because the selected loops have highly conserved sequences (Fig. 1A), we tested whether the antibodies generated against the meningococcal antigens could block ligand binding in the gonococcus. We implemented a solid-phase binding assay with whole iron-stressed gonococci to address this question. We first demonstrated the specificity of this assay by showing that unlabeled hTf, but not bTf, was capable of blocking the deposition of HRP-Tf (Fig. 3A). We then determined that the loop antibodies alone and in combination were unable to substantially block ligand binding (Fig. 3B). An antibody developed against full-length TbpA was capable of modest blocking. These conclusions were further supported by antibody-mediated ligand-blocking ELISAs (Fig. 3C). When quantified, none of the antibodies was capable of accomplishing greater than 20% inhibition of ligand binding on the gonococcal surface. Interestingly, the antibodies had a greater inhibitory effect on the *E. coli* strain overexpressing TbpA. This phenomenon was more pronounced when evaluating the effects of the holo-TbpA antibody, which inhibited only 13% of the ligand binding in the gonococcus but resulted in an 85% reduction in ligand binding in *E. coli*. With the evidence that these loop antibodies were insufficient to significantly abrogate ligand binding, TbpA loop antibodies were regenerated by a different approach in an effort to optimize their inhibitory characteristics.

Antibodies raised against cyclized TbpA loop peptides demonstrate modest Tf blocking on whole cells. In reviewing the way the original TbpA loop antibodies were designed, several areas for improvement were discovered. The first was that the linear epitopes may not have taken on the appropriate three-dimensional (3D) conformation required to target surface-exposed, folded TbpA. The second was that the antibodies were developed against peptides with an *N. meningitidis* sequence that is not identical to the gonococcal sequence (Fig. 1), particularly in loop 7. Lastly, the peptide fragments were short, often less than half the length of the entire surface-exposed loop. In the redesign of the loop antibodies, all three of these concerns were addressed. The peptides were designed to contain gonococcal sequence, were substantially extended in length, and were cyclized by adding cysteine residues to both ends (Table 2). Mice were immunized subcutaneously with TiterMax as the adjuvant, and boosters were given at days 21 and 42. On the first attempt, titers for loop 7- and loop 11-derived antibodies were robust but loop 3 was found to be poorly immunogenic. After analysis of the peptide sequence for major histocompatibility complex class II epitopes, the loop 3 peptide had a weaker score than the other loop peptides. A second attempt at loop 3 peptide immunization was performed by adding ovalbumin to the peptide and TiterMax adjuvant, which resulted in improved titers. With the new sera (second generation), the solid-phase ligand-blocking assay described above was repeated. Despite the additional considerations applied to their design, the second-generation antibodies showed no detectable ligand-blocking ability (Fig. 4A). Again, these results were supported by antibody-mediated ligand-blocking ELISAs (Fig. 4B). The second-generation antibodies had effects comparable to those of the original antibodies (Fig. 3C) on the gonococcal surface, with 11 to 17% reductions in ligand binding. However, the redesigned antibodies had less of an inhibitory effect on the recombinant TbpA-overexpressing *E. coli* strain. Although no greater inhibitory effect

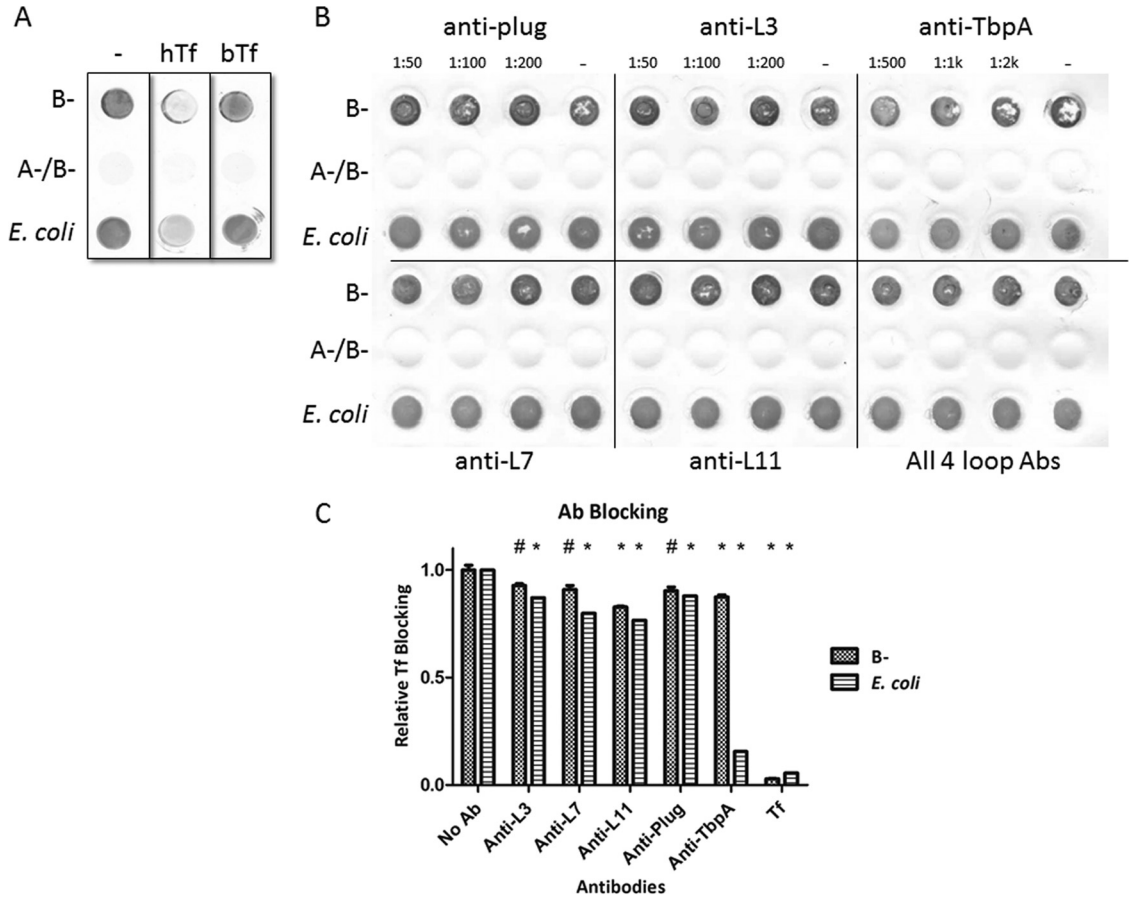

FIG 3 Solid-phase antibody-mediated ligand-blocking assays. Whole iron-stressed gonococci or *E. coli* cells expressing recombinant TbpA were applied to a nitrocellulose membrane and allowed to dry. (A) Blots were blocked with either 20 μg/ml hTf or bovine Tf (negative control), and then HRP-Tf was applied. After washing, HRP was detected with Opti-4CN (Bio-Rad). The positive control (lane −) contains no blocking agent and therefore represents maximal hTf binding. (B) Blots were blocked with antibodies (Abs), and then HRP-Tf was applied. Peroxidase activity was detected with Opti-4CN. Also tested was an antibody raised against full-length TbpA (anti-TbpA). The negative controls are strains from which TbpA is absent (A−/B−). (C) A similar assay was performed with whole cells in a microtiter dish for an ELISA. 3,3′,5,5′-Tetramethylbenzidine (Thermo) was used as the peroxidase substrate, and the OD_{420} was measured. The positive control is the condition without antibody (No Ab), and the negative control is incubation with unlabeled Tf. The data are the specific binding calculated by subtracting values obtained from strains without Tf receptors from those from the experimental strains. Significant differences are noted (*, $P < 0.01$; #, $P < 0.05$). Statistics were calculated with the Student *t* test.

was obtained with the redesigned antibodies, these data suggest that there are differences in the presentation of TbpA between *E. coli* and the gonococcus, which should be taken into consideration in future studies. Having addressed the interaction of loop-specific antibodies with the native bacterium, we shifted the focus to probing the structure-function properties of the loop 3 helix of TbpA, which was hypothesized to be a key functional domain.

Loop 3 helix mutant TbpA proteins are impaired for Tf binding and iron uptake in the absence of TbpB. Within the iron chelation center in Tf, a triad of pH-sensing residues has been shown previously to control iron binding affinity (19, 37). The crystal structure of TbpA suggests that a polar residue on the loop 3 helix might be able to destabilize the triad's charge balance in Tf, leading to iron release. To test this hypothesis, substitution mutations for all of the polar residues on the loop 3 helix were created (Fig. 5; Table 3). For all of the newly created mutants, TbpA expression was determined to be equal to that of the WT by Western blotting (see Fig. S1 in the supplemental material). As the first metric of protein function, we assessed the ability of mutagenized TbpA to bind to its ligand, hTf. In order to detect a binding defect specific for TbpA, whole-cell ELISAs with TbpB-deficient strains were implemented. In these assays, there were two negative controls. The "Comp" condition (Fig. 6), or competitive inhibition, contained excess unlabeled hTf applied with HRP-labeled Tf. The 6905 L3HA condition contains a *tbpB* deletion strain that simultaneously has a hemagglutinin (HA) epitope insertion in TbpA loop 3. This strain has been previously shown to be incapable of binding hTf (23). In this study, we determined that the singly substituted TbpA proteins were able to bind Tf at 40 to 80% of the WT level, while the loop 3 helix deletion (L3HΔ) mutant bound Tf

TABLE 2 Sequences of peptide used for second-generation immunizations

Loop	Sequence
3	CTKAVFDANQKQAGSLRGNGKYAGNHKC
7	CRLPSFAEMYGWRSGDKIKAVKIDPC
11	CRYVTWENVRQTAAGAVNQHKNVGVYNRYAAPGRC

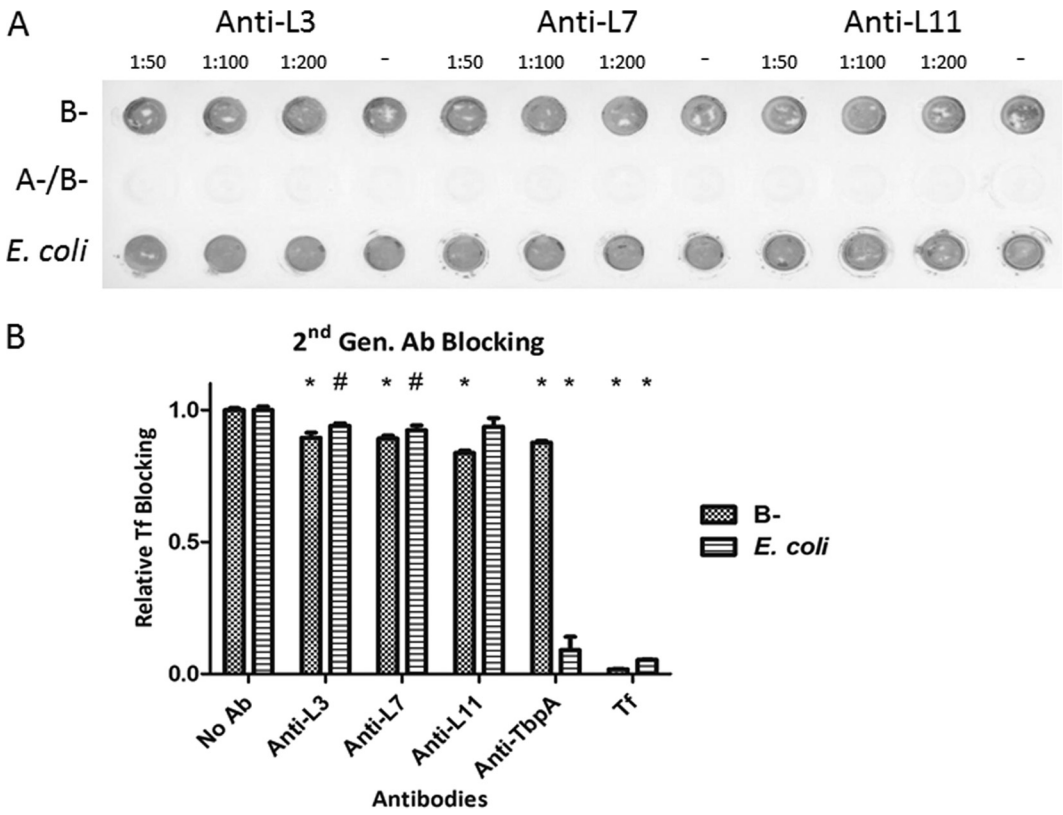

FIG 4 Antibody-mediated ligand-blocking assays for second-generation loop-specific antibodies. Whole, iron-stressed gonococci or *E. coli* cells expressing recombinant TbpA were applied to a nitrocellulose membrane and allowed to dry. (A) To determine loop antibody-blocking capability, blots were blocked with antibodies and then HRP-Tf was applied. For both blots, HRP was detected with Opti-4CN. Lane – contained no antibody and therefore represents the maximal amount of hTf bound. (B) A similar assay was performed with whole cells in a microtiter dish for an ELISA. 3,3′,5,5′-Tetramethylbenzidine (Thermo) was used as the peroxidase substrate, and the OD_{420} was measured. The positive control is the condition without antibody (No Ab), and the negative control is incubation with unlabeled hTf (Tf). The data represent specific binding obtained by subtracting the values obtained with strains without Tf receptors from those obtained with the experimental strains. Significant differences are noted (*, $P < 0.01$; #, $P < 0.05$). Statistics were calculated with the Student *t* test.

at approximately 9% of the WT level (Fig. 6). Next, the ability of each mutated TbpA protein to mediate iron internalization was quantified with a radiolabeled iron uptake assay. This assay employed the same 6905 L3HA strain as a negative control. In these experiments, we determined that the singly substituted TbpA proteins were able to internalize iron at 14 to 47% of the WT level, while the loop 3 helix deletion mutant internalized iron at <1% of the WT level (Fig. 7). These data demonstrate that all of the single residue mutations substantially impacted TbpA function.

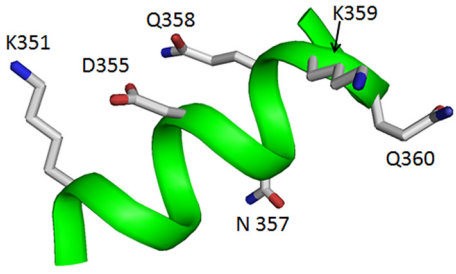

FIG 5 Loop 3 helix polar residues. Loop 3 helix with all polar residues displayed as stick models. All residues displayed were mutagenized for this study as listed in Table 2.

TbpB expression enables iron internalization in the loop 3 helix mutant TbpA proteins. We next assessed whether TbpB was able to restore the iron uptake function in strains with a defective TbpA transport protein, as this phenomenon was observed in our previous study (23). This hypothesis was tested with a subset of the isogenic TbpA mutants, coexpressing functional TbpB, in the radiolabeled iron uptake assay described above. In the presence of TbpB, all of the point mutants demonstrated greatly increased iron uptake, to 70 to 98% of the WT level (Fig. 8). The helix deletion strain, however, continued to demonstrate a severe defect, with iron uptake below 5% of the WT level. The range of

TABLE 3 Mutagenesis of helix residues[a]

Position	Wild type	Mutation(s)
351	Lysine	Ala
355	Aspartic acid	Ala, Lys
357	Asparagine	Ala
358	Glutamine	Ala
359	Lysine	Ala, Glu Acid, Arg
360	Glutamine	Ala, Glu Acid, Lys

[a] Shown are the polar TbpA loop 3 helix residues by amino acid position. Each point mutation created is adjacent to the wild-type residue. All residues were mutagenized to alanine, and some were additionally changed to like or opposite charges.

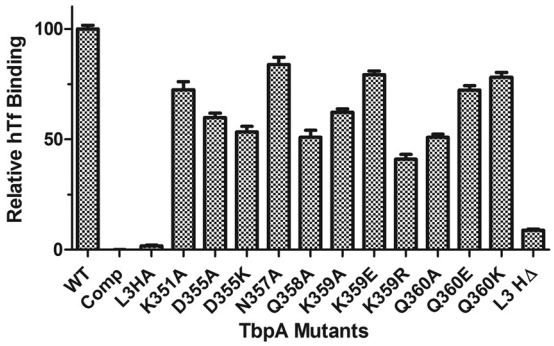

FIG 6 TbpA-Tf binding ELISAs of TbpB$^-$ strains. Whole, iron-stressed, TbpB-deficient gonococcal cells were applied to microtiter dishes for ELISAs with HRP-labeled Tf as the ligand. FA6905 (WT) served as the positive control, and FA6905 L3HA (L3HA) and the excess competitor hTf condition (Comp) served as negative controls. All data were normalized to FA6905. The data represent the mean values ± standard errors of at least three independent binding experiments. For all of the mutants compared to the positive control, the *P* values are <0.001, with the exception of the Q360K mutant, where the *P* value is <0.01. Statistics were calculated with the Student *t* test.

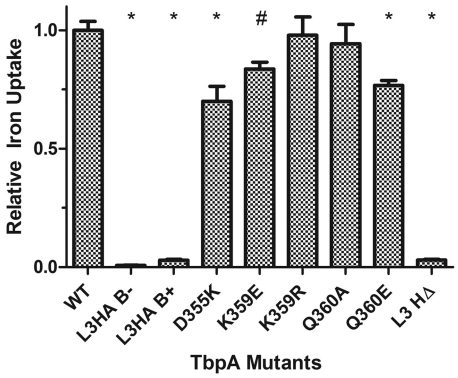

FIG 8 Iron internalization by TbpB-expressing strains. Whole, iron-stressed gonococcal cells were applied to microtiter dishes for radiolabeled iron uptake assays. Iron uptake was calculated as counts per microgram of protein. The amount of iron internalized was determined by subtracting the counts obtained with KCN from those generated with metabolically active cells. Internalized counts were then normalized to that of FA19 (WT TbpA). FA19 (WT) served as the positive control, and FA6905 L3HA (L3HA, B−) and FA19 L3HA (L3HA, B+) served as negative controls. The data represent the mean values ± standard errors of at least three independent binding experiments. Significant differences are noted (*, $P < 0.001$; #, $P < 0.01$). Statistics were calculated with the Student *t* test.

defects seen in the Tf-binding ELISA and the iron uptake assays were quite varied for single residue substitutions, but no information about the ability to survive on Tf as the sole iron source can be derived from these experiments. We therefore set out to determine if any of the mutant TbpA proteins, in the presence or absence of TbpB, were capable of growing on iron-depleted medium supplemented with partially ferrated Tf.

Strains with TbpA loop 3 helix mutations are capable of growth on Tf as the sole iron source. In order to assess the abilities of the mutant TbpA proteins to grow on Tf as the sole iron source, we grew all 12 *tbpA* mutants, with and without functional TbpB, on GC medium agar plates. The next day, single colonies were patched onto CDM agar plates containing 10% ferrated Tf and grown for 48 h at 37°C with 5% CO_2. Since Tf in circulation in the human body is 30% ferrated, this condition represents a saturation level below that which is physiologically achieved. At 48 h, all of the strains except the negative control and the helix deletion strains were capable of growth on Tf as the sole iron source (Fig. 9).

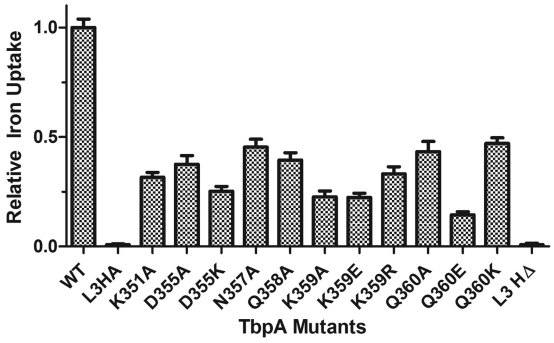

FIG 7 Iron internalization by TbpB-deficient strains. Whole, iron-stressed, TbpB-deficient gonococcal cells were applied to microtiter dishes for radiolabeled iron uptake assays. Iron uptake was calculated as counts per microgram of protein. Specific uptake was calculated by subtracting the counts obtained with KCN from those generated from metabolically active cells. Specifically internalized iron counts were then normalized to that of FA6905 (WT TbpA). FA6905 served as the positive control, and FA6905 L3HA (L3HA) and the excess competitor hTf condition (Comp) served as negative controls. The data represent the means ± standard errors of at least three independent binding experiments. For all of the mutants compared to the positive control, the *P* values were <0.001. Statistics were calculated with the Student *t* test.

TbpA in the loop 3 helix mutants is surface exposed. To confirm the surface exposure of the mutated TbpA proteins, we used a proteolytic cleavage assay on whole iron-stressed gonococci. Cells were subjected to a time course of trypsin digestion and then processed for preparation of whole-cell lysates. Whole-cell proteins were separated by SDS-PAGE and then transferred to nitrocellulose for Western blotting. The presence of TbpB did not affect the digestion pattern (Fig. 10), and all of the single residue mutants had the same digestion pattern as the WT (data for some mutants not shown). The loop 3 helix deletion strain had a similar digestion pattern, but the relative intensities of the bands were slightly affected. The digestion patterns of the single residue mutants, combined with their retention of iron uptake functions, confirm that the proteins are surface exposed and in the proper conformation. The digestion pattern of the loop 3 deletion strain is similar to that displayed by the loop 3 HA epitope insertion strain described previously (23). Although the TbpA conformation may be slightly altered in the latter two mutants, proteolysis demonstrates that the TbpA proteins are indeed surface exposed.

DISCUSSION

TbpA is considered a viable vaccine candidate for the prevention of gonococcal infection, because of its lack of antigenic and phase variation (38), but there have been complications in the development of a successful vaccine. One issue is that, when used as an immunogen, TbpA alone results in a relatively weak immune response (39, 40). In addition, although TbpA is required for initiation of human infection (20), it is not required for survival in the estradiol-treated female mouse model used for vaccine development (41, 42), complicating efforts to target TbpA alone (for a review, see reference 15). Some challenges to vaccine development were to be expected when the primary resource was a 2D topology

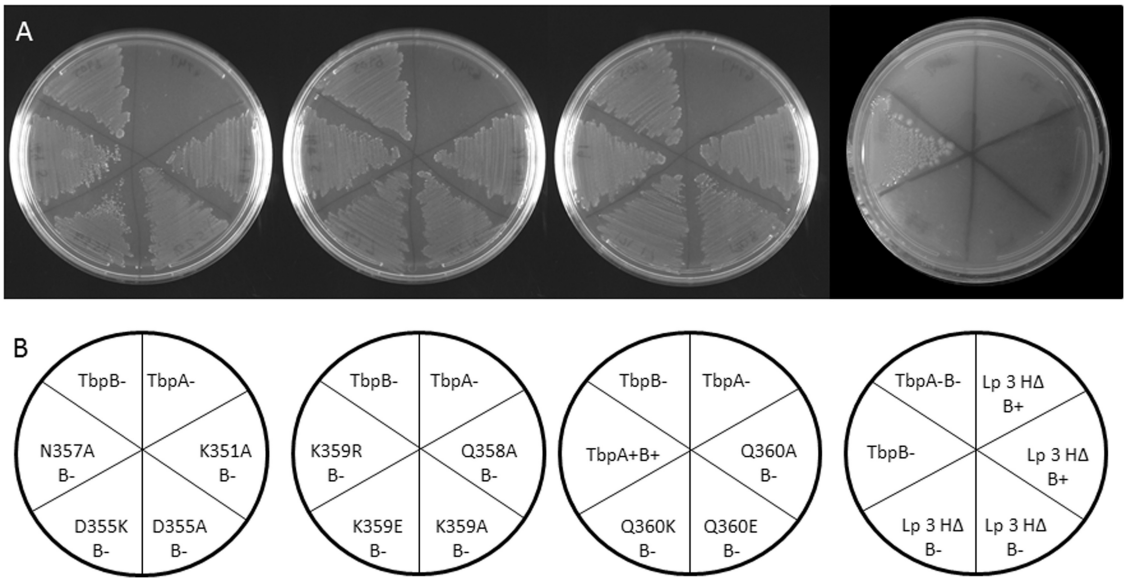

FIG 9 Growth of *tbpA* mutants on hTf as the sole iron source. (A) CDM agar plates containing 10% saturated hTf with six strains grown per plate. Each plate has FA6905 as a positive control and FA6747 as a negative control in addition to several mutants with point mutations. (B) Plate layout diagram describing the phenotypes of the strains streaked on the sectors of the plates above.

map of TbpA that took over a decade of work to refine (43). However, there were hopes that once a 3D structure was developed, it would greatly accelerate the ability to target key regions of TbpA for vaccine development. With the resolution of the crystal structure of TbpA from *N. meningitidis* in 2012, which largely confirmed the 2D topology model in the gonococcus, it was anticipated that these data would be invaluable for gonococcal studies because of the high sequence homology between the related pathogens. After solving the structure, Noinaj et al. developed antibodies against four small predicted functional domains of the protein (21). In recombinant *E. coli*, these antibodies showed some promise, although the sera had to be used at high concentrations (1:20) to demonstrate any inhibitory effect. These crystal structure-derived epitopes showed potential, but they were not tested in the native bacterium.

We set out to bridge the gap in our understanding of antibody interactions by using *N. gonorrhoeae* versus recombinant *E. coli*. Using the antibodies from the previously mentioned study, we determined that, when applied to the gonococcus, these antibodies did not interact with TbpA in the same manner that they did for recombinant *E. coli*. In fact, the antipeptide antibodies were twice as effective against *E. coli* in some cases and even then demonstrated only a modest ability to block TbpA-ligand interactions. It is possible that these antibodies did not block the ligand well because the immunogens were too small to elicit robust titers. We have determined previously that antibodies raised against larger loop antigens for loops 2, 4, and 5 can bind to the gonococcal surface (44). However, even these longer loop-specific antibodies were unable to block Tf binding (44). Another possible explanation for why the original loop antibodies did not block TbpA-ligand interactions is that the linear presentation of the peptide immunogens may not have represented the structural complexity

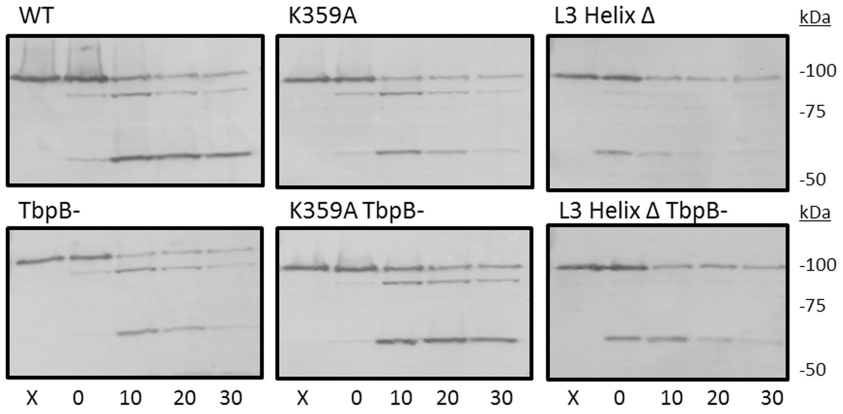

FIG 10 TbpA mutations do not prevent surface exposure. Whole, iron-stressed gonococcal cells were exposed to trypsin for 0, 10, 20, and 30 min, after which the reaction was stopped by the addition of aprotinin. Lanes X were not treated with trypsin. Bacteria were pelleted, subjected to SDS-PAGE, and then transferred to nitrocellulose. Western blots were probed with polyclonal TbpA antibody. Full-length TbpA is 100 kDa. Trypsin cleavage resulted in TbpA fragments of approximately 95 and 55 kDa.

of the loops in their native context, resulting in decreased binding to folded TbpA. These unanticipated findings demonstrate the complexity of the development of immunogens specifically from the crystal structure alone. However, by using length, composition, and conformation modifications, we were able to make second-generation TbpA loop-specific antibodies that we predicted could overcome some of the limitations of the original loop antibodies. Although similar levels of ligand blocking were demonstrated with these new antibodies on the gonococcal surface, there was an observed decrease in efficacy against *E. coli*. This finding presents new questions about effective antibody development. Further work needs to be done to investigate the roles of various loops, explore how peptide presentation translates to antibody efficacy, and determine why some antibodies, like the holo-TbpA antibodies, are effective against *E. coli* but not the gonococcus. Despite these lingering questions, this work's innovative approach to the development of peptide-specific antibodies will provide helpful insights for future work targeting the Tbp proteins for vaccine development.

After antibody function on the gonococcal surface was addressed, attention was shifted to further exploration of the structure-function relationships predicted for TbpA. On the basis of our previous studies, we concluded that HA tag insertion into loop 3 completely inactivated TbpA function (23). The TbpA crystal structure also shows that the loop 3 helix seems to fit inside the C-lobe cleft of Tf, in close proximity to the iron chelation center. Within this chelation center, there is a triad of pH-sensing residues (K534, R632, and D634) that are predicted to control iron binding and release. TbpA residue K359 is adjacent to this triad and was hypothesized to disrupt the charge balance enough to release the iron from the coordinating residues. To test this hypothesis, mutations were made to change each of the polar residues on the helix. A complete helix deletion was also generated. Gonococcal strains that had these TbpA mutations with and without the coreceptor, TbpB, were created so that effects on TbpA could specifically be evaluated. Finally, the phenotypes of the mutants were determined in the two steps of the TbpA-Tf interaction: ligand binding and iron extraction/internalization.

We assessed mutant TbpA-Tf binding by using ELISAs and determined that, in the absence of the coreceptor, there was a moderate reduction in ligand binding. The helix deletion strain, however, suffered a severe reduction in binding, suggesting that the entire helix domain is important for ligand interaction. Although single residue mutations had only modest effects, there are 81 predicted TbpA residues that interact with Tf, so it was unlikely that any single residue mutation would completely abrogate TbpA-Tf binding. Although interference with ligand binding was a promising outcome, assessment of iron uptake was the primary objective and was more likely to be affected by the mutations selected.

We proceeded to analyze the abilities of the mutant TbpA proteins to utilize Tf-bound iron with a radiolabeled iron uptake assay. As predicted, the iron uptake function was impacted more than ligand binding, supporting our hypothesis that loop 3 helix polar interactions are involved in iron release from its chelation center in Tf. Mutation of the polar residues all along the helix had substantial negative effects, but certain residues stood out as more important than others. As mentioned previously, it was predicted that the lysine residue at TbpA position 359 was the key residue in contributing to iron release. Indeed, when this residue was mutated to residues with the opposite or no charge, some of the most substantial decreases in iron uptake occurred. Surprisingly, the greatest decrease in protein function came from an additional negative charge at residue 360. Together, these data suggest that a positive charge in the Tf C-lobe cleft is required to cause iron release and utilization. Additionally, changing the identities of all of the residues tested along the length of the helix caused a >50% reduction in protein function. This implies that all of these residues are required to position the helix properly in the cleft for optimal functioning. This concept is further supported by the loop 3 helix deletion strain, which was incapable of iron internalization.

Although it is easiest to see defects when evaluating TbpA alone, this is not a realistic view of how the Tf iron acquisition system functions in the gonococcus. Indeed, no TbpB-deficient gonococcal strains have ever been identified. Therefore, we repeated the radiolabeled iron uptake assays in the presence of the coreceptor TbpB with some of the best and worst performers from the TbpA-only iron uptake study. In each case, a dramatic recovery of iron uptake function was observed, although the uptake function of some of the mutants was still significantly lower than that of the WT. This might have been anticipated for several reasons. First, previous studies have demonstrated that the Tf receptor complex is relatively insensitive to point mutations (19, 21). Second, it has been hypothesized that TbpB causes a closure of the chamber formed between Tf and TbpA, so that free iron cannot diffuse away. Third, it is predicted that TbpB is largely responsible for the release of deferrated Tf. Together, this suggests that even if the Tf-iron transporter is greatly handicapped, TbpA can still accomplish its goal of sufficient nutrient acquisition if the coreceptor is present. The exception to this, again, is the helix deletion strain. This TbpA mutant has almost no capacity to internalize iron, even in the presence of TbpB. Because this mutant binds Tf at less than 10% of the WT level, it is difficult to assess whether TbpB truly cannot compensate for the defect or if the three-part complex never forms. In sum, these findings highlight the importance of the loop 3 helix motif in iron acquisition and demonstrate the likely importance of the simultaneous targeting of both Tf receptors to achieve maximal inhibition.

We were able to partially inactivate the Tf receptor complex by using mutations; therefore, we next tested whether these mutations similarly inhibited gonococcal growth on hTf as the sole iron source. When the mutant strains were grown on CDM-Tf agar plates, we found that all of the single residue mutants with and without TbpB could grow. The only strains unable to grow were the helix deletion strains. These findings suggest that even with TbpA function as low as 15% of the WT level, the gonococcus is able to survive on poorly saturated Tf as the sole iron source. The helix deletion strains demonstrate that there is a level at which growth cannot be sustained, and the level exists somewhere between 3 and 15% TbpA function. These data are novel in that they are the first to report the degree to which TbpA needs to be impaired in order to prevent growth on hTf. These data also provide new insights into the function of the loop 3 helix and further indicate that while residue K359 is important for TbpA function, other helix residues apparently play equally important roles.

We confirmed that the mutants constructed in this study were still surface exposed and folded properly. With a proteolytic accessibility assay, it was demonstrated that all of the single residue mutations, both in the presence and in the absence of TbpB, dis-

played the same cleavage pattern as the parental strain. The helix deletion strain was protease accessible, demonstrating that it was surface exposed, but the relative intensities of the cleavage products were slightly altered. This suggests that the presentation might be slightly different from that of the WT protein. Indeed, previous insertions into loop 3 demonstrated the same protease sensitivity pattern, showing that moderate perturbation of the loop potentially alters its conformation slightly.

This study demonstrates that, in the case of TbpA, structure-driven epitope selection for vaccine development does not necessarily translate into successful binding to the surface of the native bacterium. We found that loop 3 was poorly immunogenic, supporting the hypothesis that the gonococcus has evolved to keep functional domains from being targeted by the immune system (45). We also clearly demonstrated that the loop 3 helix plays a critical role in protein function, both in binding and in iron extraction/internalization. Of note, the function of the loop 3 helix was not solely dependent on K359 as predicted. Instead, all of the residues targeted for mutagenesis play important roles in TbpA function. We determined that the coreceptor TbpB can largely compensate for mutations in TbpA and that the provision of functional TbpB is sufficient to allow growth even with greatly reduced TbpA functionality.

Our studies demonstrate that more complex approaches are needed to develop efficacious, protective vaccines. The next steps may require inactivation of ligand binding functions in order to increase immunogenicity, thus making our ongoing structure-function analyses even more critical. Beernink et al. demonstrated that ligand binding-deficient factor H binding protein (fHbp) from *N. meningitidis* was as immunogenic as the WT protein but produced higher serum bactericidal activity (SBA) titers when introduced into transgenic mice expressing human fH (46). Rossi et al. went on to investigate subfamily A fHbp, which has two distinct point mutations that decrease fH binding. Immunization with this protein led to significantly higher IgG titers and SBA responses in human fH transgenic mice (47). The phenomenon of ligand binding resulting in decreased immunogenicity was also seen to a lesser degree in rhesus macaques (48). Recently, similar results were described for TbpB in *Haemophilus parasuis* (24).

The studies described in this report represent the first gonococcal structure-function characterization of the Tf receptor system since it was crystallized from *N. meningitidis* in 2012. The resolution of these crystal structures provides critical information to the field, serves as a foundation for studies like those described here, and represents the start of a new era in the pursuit of vaccine development and therapeutic intervention efforts targeting these proteins. Future work will examine loop 3 helix mutant TbpA proteins for immunogenicity in the presence and absence of human Tf. Other important studies include structure-based screening studies to identify potential small-molecule inhibitors of the TbpA-Tf interaction. Inhibitory compounds could represent very specific therapeutic treatments for gonococcal disease or may be employed as adjuncts to traditional antimicrobial therapies.

ACKNOWLEDGMENTS

Funding for this work was provided to C.N.C. by Public Health Service grants R01 AI065555, R01 AI084400, and U19 AI31496 from the National Institute of Allergy and Infectious Diseases, National Institutes of Health. D.R.C. was supported by fellowship grant F30 AI112199 from the National Institute of Allergy and Infectious Diseases, National Institutes of Health. N.N. and S.K.B. were supported by the intramural research program of the NIH National Institute of Diabetes and Digestive and Kidney Diseases.

We thank Herman Staats at Duke University for his assistance with immunogen selection and consultation related to adjuvants. We also are grateful to Greg Simpowski and Melissa Ventevogel at Duke University for development of the second-generation antipeptide mouse antiserum. We thank Karen Ostberg for the creation of pVCU757. We acknowledge the efforts of Shelby Daniel-Wayman and Michael Brady as summer interns on this project.

REFERENCES

1. **Walker CK, Sweet RL.** 2011. Gonorrhea infection in women: prevalence, effects, screening, and management. Int J Womens Health **3:**197–206.
2. **World Health Organization.** 2008. Global incidence and prevalence of selected curable sexually transmitted infections—2008. World Health Organization, Geneva, Switzerland. http://apps.who.int/iris/bitstream/10665/75181/1/9789241503839_eng.pdf.
3. **Centers for Disease Control and Prevention (CDC).** 2011. Cephalosporin susceptibility among *Neisseria gonorrhoeae* isolates—United States, 2000–2010. MMWR Morb Mortal Wkly Rep **60:**873–877.
4. **Liu Y, Feinen B, Russell MW.** 2011. New concepts in immunity to *Neisseria gonorrhoeae*: innate responses and suppression of adaptive immunity favor the pathogen, not the host. Front Microbiol **2:**52.
5. **Farley TA, Cohen DA, Elkins W.** 2003. Asymptomatic sexually transmitted diseases: the case for screening. Prev Med **36:**502–509. http://dx.doi.org/10.1016/S0091-7435(02)00058-0.
6. **Centers for Disease Control and Prevention (CDC).** 2007. Update to CDC's sexually transmitted diseases treatment guidelines, 2006: fluoroquinolones no longer recommended for treatment of gonococcal infections. MMWR Morb Mortal Wkly Rep **56:**332–336.
7. **Ohnishi M, Golparian D, Shimuta K, Saika T, Hoshina S, Iwasaku K, Nakayama S, Kitawaki J, Unemo M.** 2011. Is *Neisseria gonorrhoeae* initiating a future era of untreatable gonorrhea?: detailed characterization of the first strain with high-level resistance to ceftriaxone. Antimicrob Agents Chemother **55:**3538–3545. http://dx.doi.org/10.1128/AAC.00325-11.
8. **Ohnishi M, Saika T, Hoshina S, Iwasaku K, Nakayama S, Watanabe H, Kitawaki J.** 2011. Ceftriaxone-resistant *Neisseria gonorrhoeae*, Japan. Emerg Infect Dis **17:**148–149. http://dx.doi.org/10.3201/eid1701.100397.
9. **Unemo M, Golparian D, Nicholas R, Ohnishi M, Gallay A, Sednaoui P.** 2012. High-level cefixime- and ceftriaxone-resistant *Neisseria gonorrhoeae* in France: novel *penA* mosaic allele in a successful international clone causes treatment failure. Antimicrob Agents Chemother **56:**1273–1280. http://dx.doi.org/10.1128/AAC.05760-11.
10. **Cámara J, Serra J, Ayats J, Bastida T, Carnicer-Pont D, Andreu A, Ardanuy C.** 2012. Molecular characterization of two high-level ceftriaxone-resistant *Neisseria gonorrhoeae* isolates detected in Catalonia, Spain. J Antimicrob Chemother **67:**1858–1860. http://dx.doi.org/10.1093/jac/dks162.
11. **Lahra MM, Ryder N, Whiley DM.** 2014. A new multidrug-resistant strain of *Neisseria gonorrhoeae* in Australia. N Engl J Med **371:**1850–1851. http://dx.doi.org/10.1056/NEJMc1408109.
12. **Briat JF.** 1992. Iron assimilation and storage in prokaryotes. J Gen Microbiol **138:**2475–2483. http://dx.doi.org/10.1099/00221287-138-12-2475.
13. **Neilands JB.** 1981. Microbial iron compounds. Annu Rev Biochem **50:**715–731. http://dx.doi.org/10.1146/annurev.bi.50.070181.003435.
14. **Cornelissen CN, Hollander A.** 2011. TonB-dependent transporters expressed by *Neisseria gonorrhoeae*. Front Microbiol **2:**117.
15. **Cornelissen CN.** 2008. Identification and characterization of gonococcal iron transport systems as potential vaccine antigens. Future Microbiol **3:**287–298. http://dx.doi.org/10.2217/17460913.3.3.287.
16. **Mickelsen PA, Blackman E, Sparling PF.** 1982. Ability of *Neisseria gonorrhoeae*, *Neisseria meningitidis*, and commensal *Neisseria* species to obtain iron from lactoferrin. Infect Immun **35:**915–920.
17. **Biswas GD, Anderson JE, Sparling PF.** 1997. Cloning and functional characterization of *Neisseria gonorrhoeae tonB*, *exbB* and *exbD* genes. Mol Microbiol **24:**169–179.
18. **Anderson JE, Leone PA, Miller WC, Chen C, Hobbs MM, Sparling PF.** 2001. Selection for expression of the gonococcal hemoglobin receptor during menses. J Infect Dis **184:**1621–1623. http://dx.doi.org/10.1086/324564.

19. **Noinaj N, Buchanan SK, Cornelissen CN.** 2012. The transferrin-iron import system from pathogenic *Neisseria* species. Mol Microbiol **86:**246–257. http://dx.doi.org/10.1111/mmi.12002.
20. **Cornelissen CN, Kelley M, Hobbs MM, Anderson JE, Cannon JG, Cohen MS, Sparling PF.** 1998. The transferrin receptor expressed by gonococcal strain FA1090 is required for the experimental infection of human male volunteers. Mol Microbiol **27:**611–616. http://dx.doi.org/10.1046/j.1365-2958.1998.00710.x.
21. **Noinaj N, Easley NC, Oke M, Mizuno N, Gumbart J, Boura E, Steere AN, Zak O, Aisen P, Tajkhorshid E, Evans RW, Gorringe AR, Mason AB, Steven AC, Buchanan SK.** 2012. Structural basis for iron piracy by pathogenic *Neisseria*. Nature **483:**53–58. http://dx.doi.org/10.1038/nature10823.
22. **Calmettes C, Alcantara J, Yu RH, Schryvers AB, Moraes TF.** 2012. The structural basis of transferrin sequestration by transferrin-binding protein B. Nat Struct Mol Biol **19:**358–360. http://dx.doi.org/10.1038/nsmb.2251.
23. **Yost-Daljev MK, Cornelissen CN.** 2004. Determination of surface-exposed, functional domains of gonococcal transferrin-binding protein A. Infect Immun **72:**1775–1785. http://dx.doi.org/10.1128/IAI.72.3.1775-1785.2004.
24. **Frandoloso R, Martinez-Martinez S, Calmettes C, Fegan J, Costa E, Curran D, Yu RH, Gutierrez-Martin CB, Rodriguez-Ferri EF, Moraes TF, Schryvers AB.** 2015. Nonbinding site-directed mutants of transferrin binding protein B exhibit enhanced immunogenicity and protective capabilities. Infect Immun **83:**1030–1038. http://dx.doi.org/10.1128/IAI.02572-14.
25. **Kellogg DS, Jr, Peacock WL, Jr, Deacon WE, Brown L, Pirkle DI.** 1963. *Neisseria gonorrhoeae*. I. Virulence genetically linked to clonal variation. J Bacteriol **85:**1274–1279.
26. **West SE, Sparling PF.** 1987. Aerobactin utilization by *Neisseria gonorrhoeae* and cloning of a genomic DNA fragment that complements *Escherichia coli fhuB* mutations. J Bacteriol **169:**3414–3421.
27. **Arnold K, Bordoli L, Kopp J, Schwede T.** 2006. The SWISS-MODEL workspace: a web-based environment for protein structure homology modelling. Bioinformatics **22:**195–201. http://dx.doi.org/10.1093/bioinformatics/bti770.
28. **Masri HP, Cornelissen CN.** 2002. Specific ligand binding attributable to individual epitopes of gonococcal transferrin binding protein A. Infect Immun **70:**732–740. http://dx.doi.org/10.1128/IAI.70.2.732-740.2002.
29. **Cornelissen CN, Biswas GD, Tsai J, Paruchuri DK, Thompson SA, Sparling PF.** 1992. Gonococcal transferrin-binding protein 1 is required for transferrin utilization and is homologous to TonB-dependent outer membrane receptors. J Bacteriol **174:**5788–5797.
30. **Blanton KJ, Biswas GD, Tsai J, Adams J, Dyer DW, Davis SM, Koch GG, Sen PK, Sparling PF.** 1990. Genetic evidence that *Neisseria gonorrhoeae* produces specific receptors for transferrin and lactoferrin. J Bacteriol **172:**5225–5235.
31. **Elkins C, Thomas CE, Seifert HS, Sparling PF.** 1991. Species-specific uptake of DNA by gonococci is mediated by a 10-base-pair sequence. J Bacteriol **173:**3911–3913.
32. **Anderson JE, Sparling PF, Cornelissen CN.** 1994. Gonococcal transferrin-binding protein 2 facilitates but is not essential for transferrin utilization. J Bacteriol **176:**3162–3170.
33. **Noto JM, Cornelissen CN.** 2008. Identification of TbpA residues required for transferrin-iron utilization by *Neisseria gonorrhoeae*. Infect Immun **76:**1960–1969. http://dx.doi.org/10.1128/IAI.00020-08.
34. **DeRocco AJ, Cornelissen CN.** 2007. Identification of transferrin-binding domains in TbpB expressed by *Neisseria gonorrhoeae*. Infect Immun **75:**3220–3232. http://dx.doi.org/10.1128/IAI.00072-07.
35. **Cornelissen CN, Anderson JE, Sparling PF.** 1997. Energy-dependent changes in the gonococcal transferrin receptor. Mol Microbiol **26:**25–35. http://dx.doi.org/10.1046/j.1365-2958.1997.5381914.x.
36. **Cornelissen CN, Sparling PF.** 1996. Binding and surface exposure characteristics of the gonococcal transferrin receptor are dependent on both transferrin-binding proteins. J Bacteriol **178:**1437–1444.
37. **Halbrooks PJ, He QY, Briggs SK, Everse SJ, Smith VC, MacGillivray RT, Mason AB.** 2003. Investigation of the mechanism of iron release from the C-lobe of human serum transferrin: mutational analysis of the role of a pH sensitive triad. Biochemistry **42:**3701–3707. http://dx.doi.org/10.1021/bi027071q.
38. **Cornelissen CN, Anderson JE, Boulton IC, Sparling PF.** 2000. Antigenic and sequence diversity in gonococcal transferrin-binding protein A. Infect Immun **68:**4725–4735. http://dx.doi.org/10.1128/IAI.68.8.4725-4735.2000.
39. **Price GA, Hobbs MM, Cornelissen CN.** 2004. Immunogenicity of gonococcal transferrin binding proteins during natural infections. Infect Immun **72:**277–283. http://dx.doi.org/10.1128/IAI.72.1.277-283.2004.
40. **Price GA, Russell MW, Cornelissen CN.** 2005. Intranasal administration of recombinant *Neisseria gonorrhoeae* transferrin binding proteins A and B conjugated to the cholera toxin B subunit induces systemic and vaginal antibodies in mice. Infect Immun **73:**3945–3953. http://dx.doi.org/10.1128/IAI.73.7.3945-3953.2005.
41. **Jerse AE, Crow ET, Bordner AN, Rahman I, Cornelissen CN, Moench TR, Mehrazar K.** 2002. Growth of *Neisseria gonorrhoeae* in the female mouse genital tract does not require the gonococcal transferrin or hemoglobin receptors and may be enhanced by commensal lactobacilli. Infect Immun **70:**2549–2558. http://dx.doi.org/10.1128/IAI.70.5.2549-2558.2002.
42. **Jerse AE, Wu H, Packiam M, Vonck RA, Begum AA, Garvin LE.** 2011. Estradiol-treated female mice as surrogate hosts for *Neisseria gonorrhoeae* genital tract infections. Front Microbiol **2:**107.
43. **Boulton IC, Yost MK, Anderson JE, Cornelissen CN.** 2000. Identification of discrete domains within gonococcal transferrin-binding protein A that are necessary for ligand binding and iron uptake functions. Infect Immun **68:**6988–6996. http://dx.doi.org/10.1128/IAI.68.12.6988-6996.2000.
44. **Masri HP.** 2003. Function and immunogenicity of individual epitopes of gonococcal transferrin binding protein A. Ph.D. dissertation Virginia Commonwealth University, Richmond, VA.
45. **Hansen JK, Demick KP, Mansfield JM, Forest KT.** 2007. Conserved regions from *Neisseria gonorrhoeae* pilin are immunosilent and not immunosuppressive. Infect Immun **75:**4138–4147. http://dx.doi.org/10.1128/IAI.02015-06.
46. **Beernink PT, Shaughnessy J, Braga EM, Liu Q, Rice PA, Ram S, Granoff DM.** 2011. A meningococcal factor H binding protein mutant that eliminates factor H binding enhances protective antibody responses to vaccination. J Immunol **186:**3606–3614. http://dx.doi.org/10.4049/jimmunol.1003470.
47. **Rossi R, Granoff DM, Beernink PT.** 2013. Meningococcal factor H-binding protein vaccines with decreased binding to human complement factor H have enhanced immunogenicity in human factor H transgenic mice. Vaccine **31:**5451–5457. http://dx.doi.org/10.1016/j.vaccine.2013.08.099.
48. **Granoff DM, Costa I, Konar M, Giuntini S, Van Rompay KK, Beernink PT.** 2015. Binding of complement factor H (FH) decreases protective anti-FH binding protein antibody responses of infant rhesus macaques immunized With a meningococcal serogroup B vaccine. J Infect Dis **212:**784–792. http://dx.doi.org/10.1093/infdis/jiv081.
49. **Mickelsen PA, Sparling PF.** 1981. Ability of *Neisseria gonorrhoeae*, *Neisseria meningitidis*, and commensal *Neisseria* species to obtain iron from transferrin and iron compounds. Infect Immun **33:**555–564.